Inorganic Chemistry

Article

pubs.acs.org/IC

Excitonic Luminescence of Hemiporphyrazines

Sabrina M. Huber, Martin S. Seyfried, Anthony Linden, and Nathan W. Luedtke*

Institute of Organic Chemistry, University of Zürich, Winterthurerstrasse 190, Switzerland, 8057

Supporting Information

ABSTRACT: Metal-free hemiporphyrazine (HpH_2) is a notoriously insoluble material possessing interesting photophysical properties. Here we report the synthesis, structure, and photophysical properties of an octahedral zinc *trans*-ditriflate hemiporphyrazine complex "$HpH_2Zn(OTf)_2$" that contains a neutral hemiporphyrazine ligand. The photophysical properties of hemiporphyrazine are largely unaffected by introduction of zinc(II) triflate, but a dramatic increase in solubility is observed. $HpH_2Zn(OTf)_2$ therefore provides a convenient model system to evaluate the impact of aggregation on the photophysical properties of hemiporphyrazine. Soluble aggregates and crystalline materials containing planar hemiporphyrazines exhibit relatively strong absorbance of visible light (450−600 nm) and red luminescence (600−700 nm). Hemiporphyrazine monohydrate ($HpH_2{\cdot}H_2O$), in contrast, has a nonplanar "saddle-shaped" conformation that exhibits very little absorbance of visible light in solution or in the solid state. Upon photoexcitation at 380 nm, $HpH_2Zn(OTf)_2$ and HpH_2 exhibit multiwavelength emissions centered at 450 and 650 nm. Emissions at 450 nm are highly anisotropic, while emissions at 650 nm are fully depolarized with respect to a plane-polarized excitation source. Taken together, our results suggest that excitonic coupling of aggregated and crystalline hemiporphyrazines results in increased absorbance and emission of visible light from $S_0 \leftrightarrow S_1$ transitions that are usually symmetry forbidden in isolated species. In contrast to previously proposed theories involving excited-state intramolecular proton transfer, we propose that the multiple-wavelength luminescent emissions of $HpH_2Zn(OTf)_2$ and HpH_2 are due to emissive S_1 and S_2 states in aggregated and crystalline hemiporphyrazines. These results may provide a better understanding of the nonlinear optical properties of these materials in solution and in the solid state.

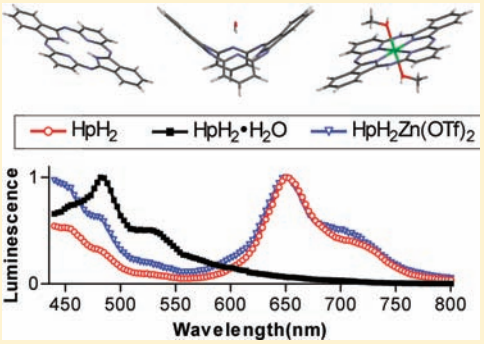

Hemiporphyrazines (Hps) were discovered more than 50 years ago,[1] but their photophysical properties remain enigmatic. Despite a relatively large body of computational results,[2−9] few experimental photophysical studies have been published.[9−14] This is due, in part, to the poor solubility properties of hemiporphyrazine free base (HpH_2) (Figure 1A) and its ability to bind water molecules to adopt nonplanar conformations with distinct photophysical properties.[4,11,15] Together with its sensitivity to acid-catalyzed hydrolysis, tendency to form aggregates, and possibility of excited-state tautomerization, these properties make metal-free hemiporphyrazines like HpH_2 very difficult to fully characterize in solution. Despite these challenges, the recent discovery of large two-photon absorption cross sections of metal-free and metallo Hps will invigorate research aimed at characterizing the basic photophysical properties of hemiporphyrazines in the solid state and in solution.[10]

In contrast to porphyrins and phthalocyanines, Hps have nonaromatic 20-electron π systems that readily adopt nonplanar conformations.[4] As a result of symmetry-forbidden $S_0 \rightarrow S_1$ transitions,[4,9] planar Hps in solution exhibit relatively weak absorbance of visible light (ε_{532nm} = 16−2800 M^{-1} cm^{-1})[1,10] but have relatively strong $S_0 \rightarrow S_2$ transitions in the far UV ($\varepsilon_{350-390nm}$ = 20 300−36 800 M^{-1} cm^{-1}).[1,4,9] Interestingly, the metal-free, anhydrous hemiporphyrazine free base (HpH_2) can exhibit multiple emission maxima (430 and 650 nm) upon photoexcitation at 380 nm. This "dual emission" was previously ascribed to formation of an emissive HpH_2 tautomer having a fully conjugated 20-electron π system with the loss of aromaticity of each pyridine group (Figure 1B).[6−9] Since free-base hemiporphyrazines have two sets of inequivalent inner nitrogen atoms, three tautomeric forms are theoretically possible (Figure 1A−C). Computational studies suggest that HpH_2 exists exclusively as tautomeric form "A" in the ground state, while emissive tautomers "B" and "C" are proposed to form as a result of excited-state intramolecular proton transfer (ESIPT) from S_2.[6−9] While light-induced tautomerization reactions are well-known phenomena in porphyrins and phthalocyanines,[16] the possible role of ESIPT in hemiporphyrazine photophysics has remained conjecture for over 15 years.[6−9] In light of other possible explanations for the multiwavelength emissions from HpH_2, such as the presence of excitons and/or triplet excited states,[10,17,18] we became interested in the synthesis and characterization of a metal-hemiporphyrazine containing a neutral HpH_2 ligand and a d^{10} metal ion having a defined oxidation state to serve as a nontautomerizable analog of HpH_2. Such "neutral-ligand" complexes will have two theoretically possible tautomers where the exchangeable protons are located on the peripheral

Received: August 12, 2011
Published: June 15, 2012

   dx.doi.org/10.1021/ic2017566 | *Inorg. Chem.* 2012, 51, 7032−7038

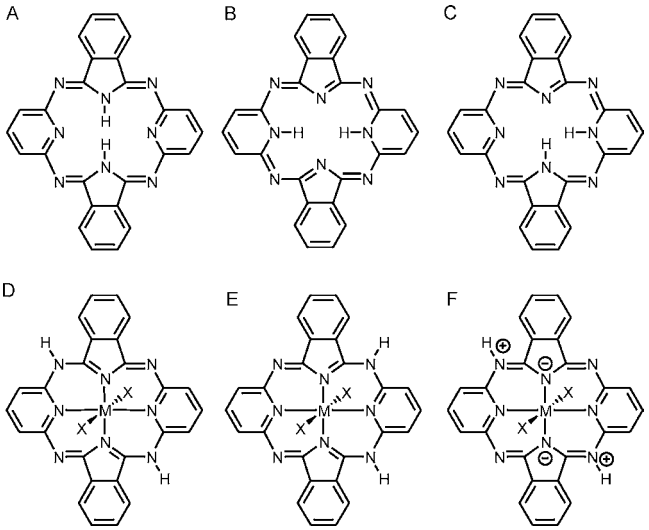

Figure 1. Possible tautomeric forms of HpH_2 (A–C) and $HpH_2M(X)_2$ in neutral (D–E) and zwitterionic (F) ligand complexes, where M = divalent metal cation and X = anion.

edge of the macrocycle (Figure 1D and 1E). Given the large distances between the sites of potential exchange, these tautomers will not undergo ESIPT. It was hitherto unknown if these types of metal complexes would exhibit multiple wavelength emission properties similar to HpH_2 and if so what the true basis of this phenomenon might be.

Here we report the synthesis and characterization of an octahedral zinc–hemiporphyrazine "$HpH_2Zn(OTf)_2$" (**1**) (Scheme 1) containing a neutral hemiporphyrazine ligand

Scheme 1. Synthesis of $HpH_2Zn(OTf)_2$

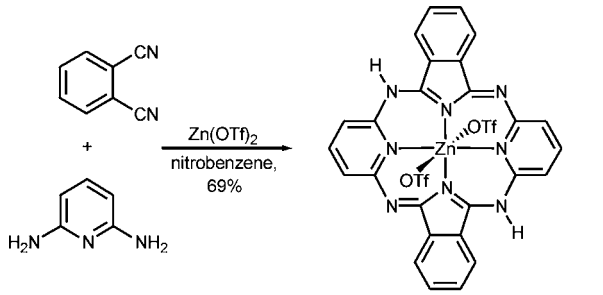

Zinc *trans*-ditriflate hemiporphyrazine
"$HpH_2Zn(OTf)_2$" (**1**)

that adopts exclusively the C_2-symmetric tautomeric form "D" in the solid state and in solution (Figure 1D). While one can consider a zwitterionic representation of the HpH_2 ligand in this complex (Figure 1F), bond length analyses indicate that the neutral representation (Figure 1D) is more informative. Unlike HpH_2 and $HpH_2{\cdot}H_2O$, $HpH_2Zn(OTf)_2$ is soluble in MeOH, DMSO, and DMF due to the presence of axial ligands on the zinc atom. The improved solubility of this complex allows for concentration-dependent analyses of its photophysical properties. Interestingly, soluble aggregates and solid-state samples of $HpH_2Zn(OTf)_2$ exhibit multiple-wavelength photoluminescence properties very similar to those of HpH_2. For both compounds in the solid state, emissions at 450 nm retain their fluorescence polarization while emissions at 650 nm are depolarized with respect to the excitation source. Taken together, our results suggest that excitonic coupling of aggregated hemiporphyrazines causes increased absorbance and emission of visible light from $S_0 \leftrightarrow S_1$ transitions that are normally symmetry forbidden in the isolated species.[4,9] While the participation of emissive triplet states cannot be excluded, we anticipate that the multiwavelength luminescence properties of $HpH_2Zn(OTf)_2$ and HpH_2 are a result of emissive $S_2 \rightarrow S_0$ and $S_1 \rightarrow S_0$ transitions. Given the growing interest in hemipophyrazine-based materials as nonlinear optical devices,[10,17,19] these results provide important design considerations by revealing the presence of excitonic luminescence in aggregated and crystalline hemiporphyrazines.

MATERIALS AND METHODS

General Methods. Phthalonitrile was purchased from Fluka; all other reagents were obtained in the highest commercially available grades from Sigma Aldrich. ^{1}H NMR spectra were measured on a Bruker ARX-300 spectrometer (Bruker, Karlsruhe, Germany). The chemical shift values are given in ppm relative to the residual signal from d_6-DMSO (δ = 2.5 ppm) or MeOD (δ = 3.31 ppm). All data processing was carried out with Topspin (Bruker). Mass spectra were measured by the Institute of Organic Chemistry at the University of Zürich. Electrospray ionization (ESI) mass spectra were measured using an Esquire-LC from Bruker. Absorbance and fluorescence spectra were measured using a Spectra Max M5 from Molecular Devices.

Synthesis of $HpH_2Zn(OTf)_2$ (1). Phthalonitrile (500 mg, 3.90 mmol), 2,6-diaminopyridine (426 mg, 3.90 mmol), and $Zn(OTf)_2$ (710 mg, 1.95 mmol) were stirred in nitrobenzene (4 mL) at 220 °C for 4 h under N_2. The reaction mixture was cooled to room temperature. The resulting precipitate was collected by vacuum filtration, repeatedly washed with CH_2Cl_2 and acetone, and dried in vacuo to yield red crystals (641 mg, 69%). ^{1}H NMR (300 MHz, MeOD): 8.20 (s br, 2 H), 8.14 (t, J = 8.0, 2 H), 7.88–7.82 (m, 8 H), 7.51 (d, J = 8.0, 4 H). Anal. Calcd for $C_{28}H_{16}F_6N_8O_8S_2Zn$: C, 41.83; H, 2.01; N, 13.94. Found: C, 41.84; H, 2.18; N, 13.96.

Synthesis of Hemiporphyrazine (HpH_2). Phthalonitrile (500 mg, 3.90 mmol) and 2,6-diaminopyridine (426 mg, 3.90 mmol) in 1-chloronaphthalene (3 mL) were heated to reflux. After 48 h the solution was cooled to room temperature. The resulting precipitate was isolated by filtration and repeatedly washed with cold methanol. After recrystallization from nitrobenzene, red needles were obtained (1.03 g, 60%). ^{1}H NMR (300 MHz, d_6-DMSO): 10.74 (s br, 2 H, NH), 7.99–7.96 (m, 4 H), 7.80–7.76 (m, 6 H); 6.84 (d, J = 7.8, 4 H). ESI MS (m/z): $[M + H]^+$ calcd for $C_{26}H_{17}N_8$, 441; found, 441.

Synthesis of Hemiporphyrazine Monohydrate ($HpH_2{\cdot}H_2O$). According to published procedures,[1] HpH_2 (50 mg, 0.11 mmol) was stirred in wet benzyl alcohol at 180 °C for 2 h. The reaction mixture was slowly cooled to room temperature over 24 h. The resulting yellow needles were isolated by vacuum filtration and dried in vacuo (51 mg, 98%).

X-ray Data Collection and Structure Determination. All measurements were made at 160 K on an Oxford Diffraction SuperNova diffractometer using Mo Kα radiation (λ = 0.71073 Å) for $HpH_2Zn(MeOH)_2{\cdot}2(OTf)$, Cu K$\alpha$ radiation (λ = 1.54178 Å) for HpH_2, and an Oxford Instruments Cryojet XL cooler. Data collection and reduction was performed with CrysAlisPro.[20] Intensities were corrected for Lorentz and polarization effects, and an absorption correction based on the multiscan method was applied. Equivalent reflections were merged. The structures were solved by direct methods using SHELXS97.[21] Least-squares refinement of each structure was carried out on F^2 using SHELXL97 with anisotropic non-hydrogen atoms.[21] OH and NH hydrogen atoms were placed in the positions indicated by a difference electron density map, and their positions were allowed to refine together with individual isotropic displacement parameters. All remaining H atoms were placed in geometrically calculated positions and refined using a riding model where each H atom was assigned a fixed isotropic displacement parameter with a

dx.doi.org/10.1021/ic2017566 | Inorg. Chem. 2012, 51, 7032–7038

value equal to $1.2U_{eq}$ of its parent C atom ($1.5U_{eq}$ for the methyl groups). Data collection and refinement parameters are given in Table 1.

Table 1. Summary of Crystallographic Data

	$HpH_2Zn(OTf)_2$	HpH_2
crystallized from	MeOH	1-methylnaphthalene
empirical formula	$C_{30}H_{24}F_6N_8O_8S_2Zn$	$C_{26}H_{16}N_8$
fw [g/mol]	868.06	440.47
cryst color, habit	red, prism	red, plate
cryst dimens [mm]	0.20 × 0.22 × 0.25	0.05 × 0.11 × 0.20
temp. [K]	160(1)	160(1)
cryst syst	triclinic	monoclinic
space group	$P\bar{1}$	$P2_1/n$
a [Å]	8.2520(2)	14.1690(4)
b [Å]	10.8769(4)	4.9988(1)
c [Å]	11.4996(5)	15.0572(4)
α [deg]	117.121(3)	90
β [deg]	95.376(2)	113.547(3)
γ [deg]	106.102(5)	90
V [Å^3]	852.88(7)	977.66(5)
Z	1	2
ρ_{calcd} [g/cm^3]	1.690	1.496
μ [mm^{-1}]	0.939	0.764
$2\theta_{(max)}$ [deg]	57	148
total reflns measd	13 290	8403
symmetry independent reflns	3780	1951
R_{int}	0.019	0.072
reflns with $I > 2\sigma(I)$	3518	1598
reflns used in refinement	3780	1951
params refined	260	158
final R(F) [$I > 2\sigma(I)$ reflns]	0.0267	0.0495
wR(F^2) (all data)	0.0703	0.1452
goodness of fit	1.059	1.036
$\Delta\rho$ (max; min) [e Å^{-3}]	0.39; −0.35	0.27; −0.30

Photophysical Measurements. *Absorbance Measurements in Solution.* Solutions of $HpH_2Zn(OTf)_2$ were prepared at a concentration of approximately 200 μM in dry methanol, and serial dilutions were conducted in a quartz cuvette with a 0.2 cm path length over the range of 200 → 25 μM. Below 25 μM, a cuvette with a 1 cm path length was used. All reported absorbance data exhibited raw absorbance values of less than 1 AU.

Absorbance Measurements in KBr. A 0.3 mg amount of each compound was ground with 200 mg of KBr in a mortar and pestle for 5 min. The resulting powder was pressed into a pellet under vacuum using a Specac 15T manual hydraulic press. The resulting pellets were 13 mm in diameter and 1 mm thick and appeared transparent to the eye. Pellets were immediately measured at an angle of 30° with respect to the incident beam.

Fluorescence Measurements in Solution. Solutions of $HpH_2Zn(OTf)_2$ were prepared at ~200 μM in dry methanol, and serial dilutions were conducted in a quartz cuvette with a 1.0 cm path length. All excitation and emission measurements were recorded at an angle of 90° with respect to the incident beam, and all raw data were corrected for inner filter effects of absorbance at each wavelength of excitation "$A(\lambda_{ex})$". Corrected values were obtained by multiplication of the raw intensity values by a correction factor "CF"

$$CF = 2.303A(\lambda_{ex})/(1 - 10^{-A(\lambda ex)}) \quad (1)$$

Fluorescence Measurements in the Solid State. Crystalline substances were ground into a powder and loaded into a polystyrene 96-well plate to a depth of approximately 0.5 mm. All excitation and emission measurements were recorded at an angle of 0° with respect to the incident beam. Emission and polarization spectra were collected by exciting the samples at 350 nm and using a long-pass emission filter at 420 nm. No correction of the raw data was conducted.

RESULTS

Synthesis and Structures. Unlike porphyrins and phthalocyanines, Hps have highly asymmetric coordination geometries. When coordinated to metals, the two nitrogen atoms from the isoindole moieties bind more tightly to the metal while the pyridine units retain much of their original character.[22,23] Previous studies have focused on the synthesis of metallohemiporphyrazines ($HpMX_n$) where the Hp ligand carries a −2 or −1 charge in complexes containing Pb(II),[1] Co(II),[11] Cu(II),[11] Ge(IV),[22] Li(I),[24] Ni(II),[25] Fe(II),[26] Mn(II),[26] Sn(IV),[27] or Cr(II).[28] In contrast, there are only a small number of reported "neutral-ligand" metallohemiporphyrazines of the type HpH_2MX_2 where M = Cu(II), Ni(II), or Zn(II) and X = Cl or Br.[5,11] In these complexes, the charge of the metal ion is balanced by the axial ligands to give a neutral HpH_2 ligand. To the best of our knowledge, no crystal structure or solid-state luminescence properties of such a complex have previously been reported.

Reactions containing a 2:2:1 mixture of 2,6-diaminopyridine, phthalonitrile, and $Zn(OTf)_2$ in refluxing nitrobenzene give a red crystalline substance $HpH_2Zn(OTf)_2$ (**1**) in ~69% isolated yields (Scheme 1). This new complex is soluble in MeOH, DMSO, and DMF, and it can be handled in the presence of oxygen and traces of water without decomposition. Crystals of $HpH_2Zn(OTf)_2$ suitable for crystallographic characterization were grown in solutions of methanol by slow diffusion of diethyl ether. Two types of crystals were obtained. The first was a relatively low-quality crystal type which gave a crystal structure consistent with elemental analysis and NMR data of $HpH_2Zn(OTf)_2$ (**1**). While reliable bond lengths cannot be ascertained from this X-ray data, the molecular framework and crystal packing of the model are dependable (Supporting Information, Figures S1 and S2). In this structure, the Hp ligand is essentially planar and the axial coordination sites of octahedral zinc are occupied by triflate ions. The second crystal type gave very high-quality diffraction data and was found to be the methanolysis product of $HpH_2Zn(OTf)_2$ where methanol had displaced the axial triflate ions from zinc. The resulting structure of the cation of "$HpH_2Zn(MeOH)_2{\cdot}2(OTf)$" is pseudo C_{2h} symmetric (Figure 2), where the two exchangeable N−H protons on the ligand are at diagonal meso nitrogen atoms. The triflate counterions (omitted for clarity in Figure 2) act as acceptors of O−H···O hydrogen bonds from methanol (H···O = 1.95(3) Å) and N−H···O hydrogen bonds from the meso nitrogen atoms (H···O = 2.13(2) Å). While one might consider a zwitterionic representation for the HpH_2 ligand in this complex (Figure 1F), bond length analyses indicate that the neutral representation (Figure 1D) is more appropriate, where the N1−C1 and N1−C4 bond lengths are highly asymmetric at 1.328(2) and 1.409(2) Å, respectively. Likewise, C1−N4 and C4−N2 are also asymmetric at 1.331(2) and 1.274(2) Å, respectively (Figure 2). These bond lengths reveal the presence of an alternating pattern of single and double bonds consistent with tautomer "D" (Figure 1D). In contrast, the structure of the free-base anhydrous ligand HpH_2 (presented below) has nearly identical N1−C1 and N1−C4 bond distances at 1.392(2) and 1.394(2) Å, respectively, and nearly identical C1−N4 and C4−N2 bond lengths at 1.282(2) and 1.276(2) Å, respectively (Figure 3). Notably, the C4−N2 double bonds and N1−C4 "single" bonds have nearly identical

dx.doi.org/10.1021/ic2017566 | Inorg. Chem. 2012, 51, 7032−7038

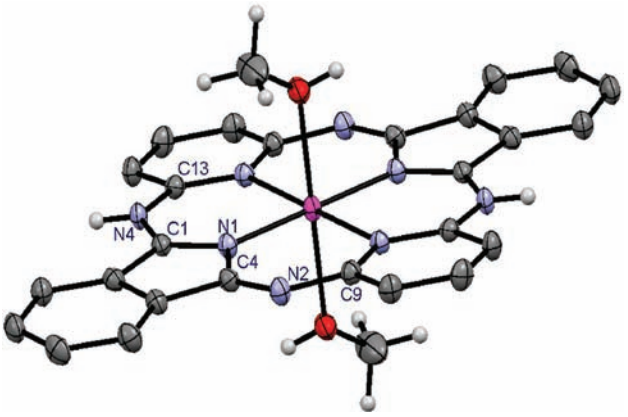

Figure 2. Crystal structure of $HpH_2Zn(MeOH)_2{\cdot}2(OTf)$ containing two equivalents of MeOH. Triflate counterions and selected hydrogen atoms have been omitted for clarity; 50% displacement ellipsoids are shown. See the Supporting Information for the lower quality crystal structure of $HpH_2Zn(OTf)_2$ (**1**) having axially coordinated triflate ions.

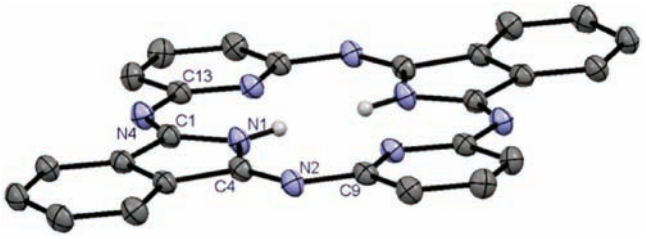

Figure 3. Crystal structure of HpH_2; 50% displacement ellipsoids are shown. Selected hydrogen atoms have been omitted for clarity.

lengths in both HpH_2 and $HpH_2Zn(MeOH)_2{\cdot}2(OTf)$. These results are consistent with the neutrality of the Hp ligand in both structures. This conclusion is further supported by the similar photophysical properties exhibited by these materials as well as the lack of acidity exhibited by $HpH_2Zn(OTf)_2$ (**1**) in methanol/water mixtures. For all experiments reported here, deprotonation of $HpH_2Zn(OTf)_2$ in solution to give an anionic ligand can be excluded, because this reaction is accompanied by a characteristic color change from red to green and the loss of solubility.[11]

Despite many decades of research, only a single, relatively low-quality crystal structure of the anhydrous hemiporphyrazine ligand (HpH_2) was available, apparently refined without hydrogen atoms (R = 0.115).[29] HpH_2 was therefore prepared according to modified published procedures,[30] and red crystals of HpH_2 suitable for single crystal X-ray diffraction were grown by slow cooling (180−25 °C) of a saturated solution in 1-methylnaphthalene under an inert atmosphere (Figure 3). The resulting structure at 160 K (R = 0.049) was found to have different unit cell parameters than the previously published structure.[29] Aside from some small distortions similar to those observed in $HpH_2Zn(MeOH)_2{\cdot}2(OTf)$, HpH_2 adopts a nearly planar structure with C_i symmetry. Despite the presence of repulsive interactions between the isoindole hydrogen atoms in the center of the macrocycle (N−H···H−N distance = 2.12(3) Å), tautomer "A" of HpH_2 is present in our crystal structure (Figures 1A and 3). The nitrogen atoms of the isoindole moieties are separated by 3.867(2) Å, while the distance between the two pyridyl nitrogen atoms is 4.506(2) Å (Figure 3). These distances are similar to those observed in $HpH_2Zn(MeOH)_2{\cdot}2(OTf)$ at 3.939(2) and 4.461(2) Å, respectively. Given the small but significant differences in bond lengths in these compounds (discussed in greater detail in the previous paragraph), it was hitherto unknown if HpH_2 and $HpH_2Zn(OTf)_2$ would exhibit similar or diverse photophysical properties. To provide a nonplanar hemiporphyrazine for comparison, we also synthesized hemiporphyrazine monohydrate ($HpH_2{\cdot}H_2O$),[1] for which a good crystallographic analysis has already been reported (Figure 4, R = 0.068).[15] This

Figure 4. Published crystal structure of $HpH_2{\cdot}H_2O$.[15]

structure is characterized by a "saddle-shaped" conformation. Interestingly, the N2−C9 bond lengths in $HpH_2{\cdot}H_2O$ of 1.411(4) Å are slightly longer than the corresponding N2−C9 bonds of 1.394(2) Å in both HpH_2 and $HpH_2Zn(MeOH)_2{\cdot}2(OTf)$. This is consistent with a greater extent of π conjugation across the pyridine units in HpH_2 and $HpH_2Zn(MeOH)_2{\cdot}2(OTf)$ as compared to $HpH_2{\cdot}H_2O$. This conclusion is supported by trends in the absorbance and fluorescence properties of these compounds.

Photophysical Properties in Solution. Solutions of 56 μM $HpH_2Zn(OTf)_2$ (**1**) in MeOH exhibit multiple emissions centered at 430 and 630 nm upon photoexciation at 380 nm (Figure 5). A similar phenomenon was reported for the

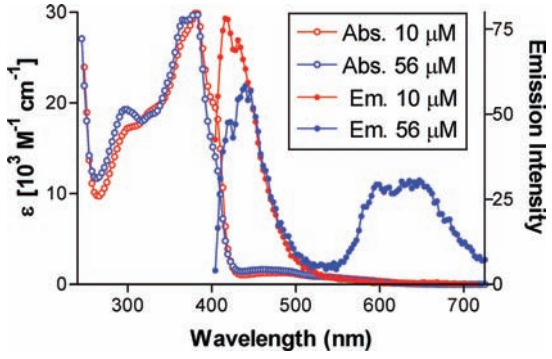

Figure 5. Absorbance (Abs) and emission (Em) spectra of $HpH_2Zn(OTf)_2$ at two different concentrations in methanol. Emission spectra were obtained using excitation at 380 nm.

anhydrous, metal-free ligand HpH_2 in DMF.[7] In our experience and those of others, crystalline HpH_2 is an insoluble material that readily converts into the nonplanar, yellow monohydrate ($HpH_2{\cdot}H_2O$) in solvents containing even small traces of H_2O.[1,11] This has a profound influence on its photophysical properties[4,9] and furthermore complicates any rigorous analysis of the concentration-dependent luminescence properties of anhydrous HpH_2 in solution. In contrast, $HpH_2Zn(OTf)_2$

dx.doi.org/10.1021/ic2017566 | Inorg. Chem. 2012, 51, 7032−7038

provides a highly soluble model complex for the neutral HpH_2 ligand to evaluate the potential impact of aggregation on the photophysical properties of planar HpH_2.

Serial dilutions of $HpH_2Zn(OTf)_2$ conducted at room temperature in MeOH revealed concentration-dependent absorbance and fluorescence spectra. With increasing concentrations of $HpH_2Zn(OTf)_2$, increased molar extinction coefficients from 430 to 500 nm were observed (Figure 6).

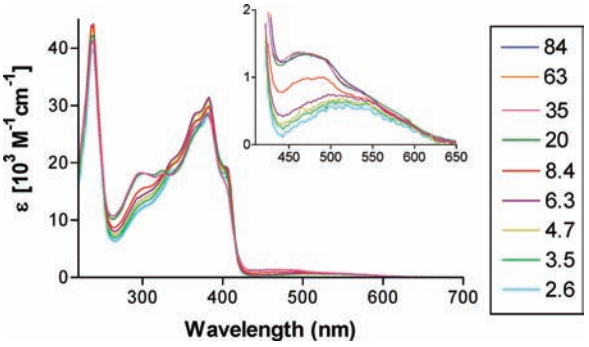

Figure 6. Absorbance spectra of $HpH_2Zn(OTf)_2$ as a function of concentration (reported in micromolar) in MeOH.

This is the same wavelength range predicted for symmetry-forbidden $S_0 \rightarrow S_1$ transitions in HpH_2.[4,9] Changes in luminescence also occur with increasing concentrations of $HpH_2Zn(OTf)_2$ in MeOH, where a linear increase in fluorescence intensity (Ex = 380 nm, Em = 450 nm) was observed from 0.1 to 5 μM, followed by a decrease in emission from 7 to 15 μM (Supporting Information, Figure S3). This type of linear increase of fluorescence followed by self-quenching is consistent with a monomer−dimer equilibrium between 0.1 and 15 μM. In contrast, no detectable fluorescence emission was observed at 600−700 nm over the same concentration range. At concentrations above 20 μM, however, a nonsaturating increase in fluorescence emission was observed at 650 nm, suggestive of aggregate formation (Figure 5 and Supporting Information, Figure S3). Concentration-dependent excitation spectra (Em = 650 nm) at concentrations above 20 μM revealed two excitation maxima centered at 350 and 450 nm (Supporting Information, Figure S4). These wavelengths are similar to those predicted for $S_0 \rightarrow S_2$ and $S_0 \rightarrow S_1$ transitions in HpH_2.[4,9]

To evaluate the potential role of aggregation in the concentration-dependent photophysical properties of $HpH_2Zn(OTf)_2$, serial dilutions were conducted in DMSO (Supporting Information, Figure S5). In contrast to the results obtained in pure methanol (Figure 6), these dilutions obeyed Beer's law over the entire visible region (Supporting Information, Figure S5). In addition, no luminescent emissions at 650 nm were observed from concentrated $HpH_2Zn(OTf)_2$ solutions prepared in pure DMSO (Supporting Information, Figure S6). To further evaluate the solvent-dependent emissions at 650 nm, 83 μM solutions of $HpH_2Zn(OTf)_2$ were monitored (Ex = 380 nm) while the solvent composition was varied from 100% methanol to 100% DMSO. With increasing DMSO concentrations, the emissions at 650 nm gradually decreased while the emissions at 430 nm dramatically increased (Supporting Information, Figure S6). Taken together, these results suggest that DMSO is able to inhibit aggregation of $HpH_2Zn(OTf)_2$ and that aggregation reactions are indeed responsible for the concentration-dependent photophysical properties of $HpH_2Zn(OTf)_2$ observed in pure methanol (Figures 5 and 6).

Photophysical Properties: Solid State. The limited solubility of HpH_2 and its tendency to bind water molecules prevent reliable concentration-dependent characterization of its photophysical properties in solution.[1,4,9,11] We therefore prepared samples in the solid state by grinding each crystalline substance with KBr and pressing pellets. Both HpH_2 and $HpH_2Zn(OTf)_2$ exhibit relatively strong absorbances between 450 and 600 nm in the solid state with distinct features at 500 and 550 nm (Figure 7). The saddle-shaped compound $HpH_2{\cdot}H_2O$, in contrast, lacks these absorbance features (Figure 7 and Supporting Information, Figure S7).

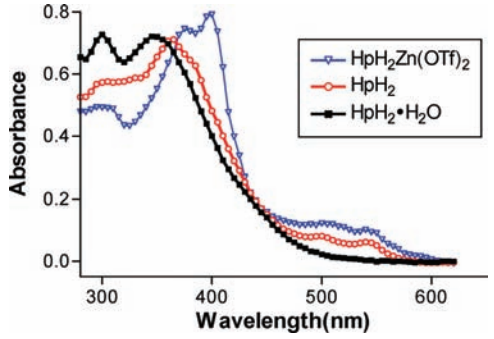

Figure 7. Absorbance spectra of $HpH_2Zn(OTf)_2$, HpH_2, and $HpH_2{\cdot}H_2O$ prepared in pressed KBr pellets at 0.3 mg/200 mg KBr with an optical path length of 1 mm. See Supporting Information Figure S7 for raw data including KBr blank.

Due to high background emissions and light scattering by KBr pellets, fluorescence emission data were collected using thick layers of neat, microcrystalline materials randomly deposited on polystyrene surfaces. Upon excitation at 350 nm, HpH_2, $HpH_2Zn(OTf)_2$, and $HpH_2Zn(MeOH)_2{\cdot}2(OTf)$ exhibit nearly identical emission spectra, with multiple emission peaks centered at 450, 480, 650, and 720 nm (Figure 8).

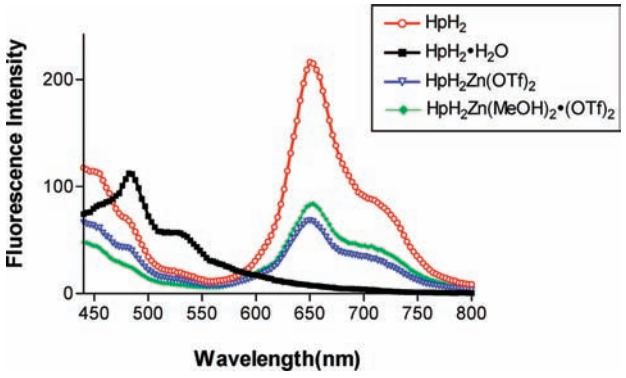

Figure 8. Fluorescence emission spectra of randomly deposited microcrystalline materials using excitation at 350 nm and a long-pass emission filter at 420 nm.

$HpH_2{\cdot}H_2O$, in contrast, exhibits multiple emission peaks centered at 450, 480, and 530 nm. Crystal packing effects have a limited influence on the photophysical properties reported here. These crystalline materials exhibit highly diverse packing geometries (Supporting Information, Figures S2 and S8−S10), but crystals of $HpH_2Zn(MeOH)_2{\cdot}2(OTf)$ and HpH_2 exhibit absorbance, emission, and polarization spectra nearly

dx.doi.org/10.1021/ic2017566 | Inorg. Chem. 2012, 51, 7032−7038

identical to that of $HpH_2Zn(OTf)_2$ (**1**) (Figures 7–9). The relative emission intensities from crystalline samples of HpH_2

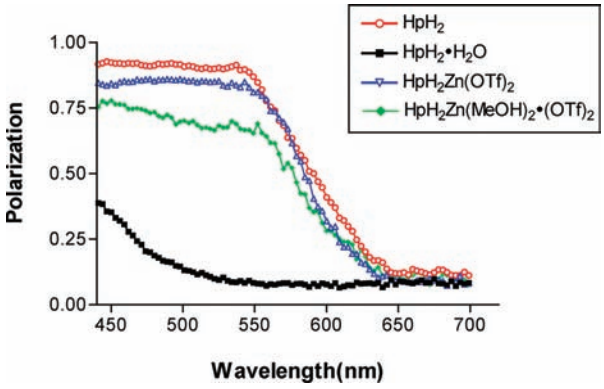

Figure 9. Fluorescence polarization of randomly deposited microcrystalline materials using excitation at 350 nm, an excitation cutoff filter at 420 nm, and plane-polarized excitation and emission with an angle of incidence = 0°. Polarization is calculated as $P = (I_v - I_h)/(I_v + I_h)$, where I_v is the intensity with parallel plane-polarized filters and I_h the intensity with perpendicular plane-polarized filters. These data have not been corrected for instrument response.

and $HpH_2Zn(OTf)_2$ at 650 nm versus 440 nm are somewhat greater for the neat materials (Figure 8) as compared to the soluble aggregates in solution (Figure 5). Together with the concentration-dependent excitation and emission observed in methanol and DMSO (Supporting Information, Figures S3, S4, and S6), these data demonstrate that the emissions at 650 nm are a result of discrete transitions present in aggregated and crystalline hemiporphyrazines.

For insight into the nature of multiple-wavelength emissions from HpH_2 and $HpH_2Zn(OTf)_2$, fluorescence emission spectra were collected using plane-polarized filters and excitation at 350 nm.[31,32] Neat samples of HpH_2, $HpH_2Zn(OTf)_2$, and $HpH_2Zn(MeOH)_2{\cdot}2(OTf)$ exhibit very similar behavior, where emissions from 400 to 550 nm are highly polarized while emissions from 650 to 700 nm are depolarized (Figure 9). Soluble aggregates of $HpH_2Zn(OTf)_2$ in methanol also give depolarized emissions at 650 nm (Supporting Information, Figure S11). Given the aggregation-dependent nature of these emissions, these polarization data suggest formation of delocalized (excitonic) excited state(s) of these materials that emit depolarized photons between 600 and 700 nm.

DISCUSSION

Due to its 20-electron, nonaromatic π system, hemiporphyrazines can readily adopt nonplanar conformations. By modulating the extent of π conjugation, the relative planarity of HpH_2 has a large influence on its photophysical properties. For example, luminescent emissions from $HpH_2Zn(OTf)_2$ and HpH_2 in the solid state (650–700 nm) are red shifted by approximately 180 nm as compared to the emissions from the nonplanar monohydrate $HpH_2{\cdot}H_2O$ (Figure 8). In addition, $HpH_2{\cdot}H_2O$ exhibits relatively little absorbance of visible light in the solid state or in solution (Figure 7 and Supporting Information, Figure S12). The planar Hp ligands present in solid-state samples of $HpH_2Zn(OTf)_2$ and HpH_2, in contrast, exhibit relatively strong absorbance from 450 to 600 nm (Figure 7). These wavelengths are similar to the "Q-band" transitions of 18 π electron porphyrins and phthalocyanines.[33–36]

The aggregation of $HpH_2Zn(OTf)_2$ has a profound impact on its photophysical properties. Upon aggregation in solution, luminescent emissions at 600–650 nm become apparent while the emissions at 400–450 nm are diminished (Figure 5 and Supporting Information, Figure S6). Previous studies have speculated that the multiple-wavelength emissions from HpH_2 are a result of excited-state intramolecular proton transfer reactions (ESIPT).[6–9] However, $HpH_2Zn(OTf)_2$ is incapable of ESIPT and yet exhibits absorbance, multiwavelength emissions, and polarization spectra very similar to those of HpH_2 (Figures 7–9). Our results therefore disprove ESIPT as the basis of the "dual-emission" properties of these compounds in the solid state.[6–9] The exact mechanism for the multiple-wavelength emissions from aggregated and crystalline hemiporphyrazines remains an open question. One possible explanation is the presence of short-lived triplet states.[10,17,18] We were unable, however, to detect any O_2 sensitivity or long-lived emissions (greater than 10 ns) from soluble aggregates of $HpH_2Zn(OTf)_2$ in solution. Another explanation is that $S_2 \rightarrow S_0$ (~450 nm) and $S_1 \rightarrow S_0$ (~650 nm) transitions are responsible for multiwavelength emissions from hemiporphyrazines. This property is already well known for porphyrins and phthalocyanines,[33–36] where aggregation has been shown to increase the $S_2 \rightarrow S_0$ or "Soret" emissions from these aromatic compounds.[34,35] Our results, in contrast, suggest a greater efficiency of $S_1 \rightarrow S_0$ emission from aggregated hemiporphyrazines. In isolation, $S_0 \leftrightarrow S_1$ transitions are normally symmetry forbidden in hemiporphyrazines,[4,9] but excitonic coupling present in aggregated and crystalline hemiporphyrazines may increase the oscillator strength of this transition due to its coupling with $S_0 \rightarrow S_2$ transitions. Porphyrins and phthalocyanines have also been shown to undergo redistribution of transition dipole strengths between their "B bands" (~400 nm) and "Q bands" (500–650 nm) upon aggregation in solution due to excitonic coupling between these transition dipoles.[31] Similar effects may be present for $HpH_2Zn(OTf)_2$, where dilute solutions exhibit strong absorbance centered at 370 nm and little, if any, absorbance at 450 nm, and aggregated samples exhibit increased extinction coefficients at 300 and 450 nm and decreased extinction coefficients from 330 to 400 nm (Figure 6). Interestingly, these changes are accompanied by the emergence of isotropic fluorescent emissions at 650–700 nm (Figures 6 and 8). Taken together, these results suggest the presence of enhanced $S_0 \leftrightarrow S_1$ transitions in aggregated hemiporphyrazines due to the presence of excitonic coupling with $S_0 \leftrightarrow S_2$ transitions.[4,9] Given the growing interest in hemipophyrazine-based materials as nonlinear optical devices,[17,19] these results provide important new design considerations by highlighting the differences in photophysical properties of planar versus nonplanar hemiporphyrazines as well as the presence of excitonic luminescence from aggregated and crystalline hemiporphyrazines.

ASSOCIATED CONTENT

Supporting Information

X-ray crystallographic data of $HpH_2Zn(MeOH)_2{\cdot}2(OTf)$ and HpH_2 in CIF format; preliminary X-ray structure of $HpH_2Zn(OTf)_2$; crystal packing diagrams and solvent-dependent absorption and emission spectra. This material is available free of charge via the Internet at http://pubs.acs.org.

dx.doi.org/10.1021/ic2017566 | Inorg. Chem. 2012, 51, 7032–7038

AUTHOR INFORMATION

Corresponding Author

*Phone: +41 44 635 4244. Fax: +41 44 635 6891. E-mail: luedtke@oci.uzh.ch.

Notes

The authors declare no competing financial interest.

ACKNOWLEDGMENTS

This work was supported by the University of Zürich and the Swiss National Science Foundation #130074.

REFERENCES

(1) Elvidge, J. A.; Linstead, R. P. *J. Chem. Soc.* **1952**, 5008−5012.
(2) Bossa, M.; Cervone, E.; Garzillo, C.; Del Re, G. *J. Mol. Struct. (THEOCHEM)* **1995**, *342*, 73−86.
(3) Honeybourne, C. L. *J. Chem. Soc., Chem. Commun.* **1972**, 213−214.
(4) Zakharov, A. V.; Stryapan, M. G.; Islyaikin, M. K. *J. Mol. Struct. (THEOCHEM)* **2009**, *906*, 56−62.
(5) Bossa, M.; Grella, I.; Nota, P.; Cervone, E. *J. Mol. Struct. (THEOCHEM)* **1990**, *210*, 267−271.
(6) Peluso, A.; Garzillo, C.; Del Re, G. *Chem. Phys.* **1996**, *204*, 347−351.
(7) Altucci, C.; Borrelli, R.; de Lisio, C.; De Riccardis, F.; Persico, A.; Porzio, A.; Peluso, A. *Chem. Phys. Lett.* **2002**, *354*, 160−164.
(8) Persico, V.; Carotenuto, M.; Peluso, A. *J. Phys. Chem. A* **2004**, *108*, 3926−3931.
(9) Bossa, M.; Cervone, E.; Garzillo, C.; Peluso, A. *J. Mol. Struct. (THEOCHEM)* **1997**, *390*, 101−107.
(10) Dini, D.; Calvete, M. J. F.; Hanack, M.; Amendola, V.; Meneghetti, M. *J. Am. Chem. Soc.* **2008**, *130*, 12290−12298.
(11) Attanasio, D.; Collamati, I.; Cervone, E. *Inorg. Chem.* **1983**, *22*, 3281−3287.
(12) Dirk, C. W.; Marks, T. J. *Inorg. Chem.* **1984**, *23*, 4325−4332.
(13) Anderson, J. S.; Bradbrook, E. F.; Cook, A. H.; Linstead, R. P. *J. Chem. Soc.* **1938**, 1151−1156.
(14) Birch, C. G.; Iwamoto, R. T. *Inorg. Chem.* **1973**, *12*, 66−73.
(15) Peng, S.-M.; Wang, Y.; Ho, T.-F.; Chang, I.-C.; Tang, C.-P.; Wang, C.-J. *J. Chin. Chem. Soc.* **1986**, *33*, 13−21.
(16) Chizhika, A. M.; Jägera, R.; Chizhika, A. I.; Bära, S.; Macka, H.-G.; Sackrowa, M.; Stanciua, C.; Lyubimtsevb, A.; Hanackb, M.; Meixner, A. J. *Phys. Chem. Chem. Phys.* **2011**, *13*, 1722−1733.
(17) Dini, D.; Calvete, M. J. F.; Hanack, M.; Amendola, V.; Meneghetti, M. *Chem. Commun.* **2006**, 2394−2396.
(18) Möllerstedt, H.; Crespo, R.; Piqueras, C.; Ottosson, H. *J. Am. Chem. Soc.* **2004**, *126*, 13938−13939.
(19) De la Torre, G.; Gray, D.; Blau, W.; Torres, T. *Synth. Met.* **2001**, *121*, 1481−1482.
(20) *CrysAlisPro*; Oxford Diffraction Ltd.: Yarnton, Oxfordshire, England, 2010.
(21) Sheldrick, G. M. *Acta Crystallogr., Sect. A* **2008**, *64*, 112−122.
(22) Esposito, J. N.; Sutton, L. E.; Kenney, M. E. *Inorg. Chem.* **1967**, *6*, 1116−1120.
(23) Sutton, L. E.; Kenney, M. E. *Inorg. Chem.* **1967**, *6*, 1869−1872.
(24) Sripothongnak, S.; Pischera, A. M.; Espe, M. P.; Durfee, W. S.; Ziegler, C. J. *Inorg. Chem.* **2009**, *48*, 1293−1300.
(25) Agostinelli, E.; Attanasio, D.; Collamati, I.; Fares, V. *Inorg. Chem.* **1984**, *23*, 1162−1165.
(26) Collamati, I.; Cervone, E.; Scoccia, R. *Inorg. Chim. Acta* **1985**, *98*, 11−17.
(27) Farris, P. J.; Jacobs, J. T.; Okonczac, M. P.; Durfee, W. S.; Noll, B. C. *Acta Crystallogr.* **1999**, *C55*, 32−33.
(28) Matassa, R.; Cervone, E.; Sadun, C. *J. Porphyrins Phthalocyanines* **2003**, *7*, 579−584.
(29) Peng, S.-M.; Wang, Y.; Chen, C. K.; Lee, J. Y.; Liaw, D. S. *J. Chin. Chem. Soc.* **1986**, *33*, 23−33.
(30) Honeybourne, C. L.; Burchill, P. *Inorg. Synth.* **1978**, *18*, 44−49.
(31) Zimmermann, J.; Siggel, U.; Fuhrhop, J.-H.; Röder, B. *J. Phys. Chem. B* **2003**, *107*, 6019−6021.
(32) Sissa, C.; Painelli, A.; Blanchard-Desce, M.; Terenziani, F. *J. Phys. Chem. B* **2011**, *115*, 7009−7020.
(33) Kobayashi, N.; Lever, A. B. P. *J. Am. Chem. Soc.* **1987**, *109*, 7433−7441.
(34) Pérez-Morales, M.; de Miguel, G.; Bolink, H. J.; Martín-Romero, M. T.; Camacho, L. *J. Mater. Chem.* **2009**, *19*, 4255−4260.
(35) Fujitsuka, M.; Won Cho, D.; Solladié, N.; Troiani, V.; Qiu, H.; Majima, T. *J. Photochem. Photobiol. A* **2007**, *188*, 346−350.
(36) Akimoto, S.; Yamazaki, T.; Yamazaki, I.; Osuka, A. *Chem. Phys. Lett.* **1999**, *309*, 177−182.